

Phonon self-energy effects in the superconducting energy gap of MgB₂ point-contact spectra

I. K. Yanson,* S. I. Beloborod'ko, and Yu. G. Naidyuk

*B. Verkin Institute for Low Temperature Physics and Engineering, National Academy of Sciences of Ukraine,
47 Lenin Avenue, 61103 Kharkiv, Ukraine*

O. V. Dolgov

Max-Planck Institut für Festkörperforschung, Stuttgart, Germany

A. A. Golubov

Faculty of Science and Technology, University of Twente, 7500 AE Enschede, The Netherlands

(Received 6 November 2003; revised manuscript received 22 December 2003; published 8 March 2004)

In strong-coupling superconductors with a short electron mean free path the self-energy effects in the superconducting order parameter play a major role in the phonon manifestation of the point-contact spectra at the above-gap energies. We derive asymptotic expressions for the nonlinear conductivity of tunnel, ballistic, and diffusive point contacts in the case $eV \gg \Delta$, and show that these expressions not only qualitatively, but also semiquantitatively correspond to the measurements of the phonon structure in the point-contact spectra for the π band of MgB₂ thin films.

DOI: 10.1103/PhysRevB.69.100501

PACS number(s): 74.70.Ad, 74.50.+r, 74.25.Fy, 73.40.Jn

I. INTRODUCTION

It is commonly accepted that the mechanism of superconductivity in recently discovered MgB₂ (Ref. 1) is due to the electron-phonon interaction (EPI) (Ref. 2). Among the known *s-p* metals, the record breaking critical temperature ($T_c \approx 40$ K) and the unusual two-band character in its electronic structure make this compound very interesting for detailed study. MgB₂ crystallizes in a hexagonal lattice with alternating planes of Mg and B. Up to now, there has been no detailed experimental determination of its EPI spectral function. The reason is that EPI in MgB₂ is strongly anisotropic, and single crystals, well suited for anisotropic measurements by means of tunneling or point-contact spectroscopy, are still under development. As for the tunneling spectroscopy, in order to extract the so-called “driving force” for high T_c in this compound caused by EPI along the *ab* plane,³ one needs a plane tunnel junction oriented perpendicular to this direction, which is not an easy task. On the other hand, the tunneling spectra in the *c* direction are supposed to be so weak (see below) that the precise standard procedure for extracting the EPI function⁴ is difficult to apply. In Ref. 5 it was shown that the inversion of the Eliashberg equation for a multiband superconductor is a mathematically ill-defined problem. The previous attempt to obtain a solution on polycrystalline samples contains an uncontrolled mixture of the two bands with a predominant contribution of the π -band.⁶ The interaction of the two bands to a great extent determines the corresponding EPI functions. Their intensity depends on electron mean free path in each band separately. On the one hand, in some experiments the two bands can be considered as being independent of each other, but, on the other hand, both of them have the same T_c , despite quite different EPI. The layered structure and strongly anisotropic EPI allow us to hope that the peculiarities in MgB₂ may shed some light on the mechanism of high- T_c superconductivity in copper oxides.

In the previous paper⁷ it was shown qualitatively that the phonon singularities in the point-contact spectra of the *c* axis oriented MgB₂ thin films were due to the nonlinear dependence of excess current $I_{exc}(eV)$ at energies higher than the superconducting energy gap Δ . In the present contribution we derive asymptotic expressions for differential conductance of *N-c-S* (*c* stands for “constriction”) point contacts and show that quantitatively (within a factor of order of unity) the calculated point-contact spectra agree with the experimental data for the *c*-axis orientation of MgB₂, where only the π band is visible.

II. THEORY

The electronic structure of MgB₂ consists of two groups of bands:^{2,3} a pair of approximately isotropic three-dimensional (3D) π bands, and a pair of strongly anisotropic 2D σ bands whose characteristics are measurable for the point contact oriented within a few degrees around the *ab* plane.⁸ As it was argued in,⁹ the variation of the superconducting gap inside the σ bands or the π bands can hardly be observed in real samples due to intraband impurity scattering. Therefore, superconducting properties of MgB₂ can be described by an effective two-band model, where each group of the σ bands and the π bands is characterized by the corresponding order parameters Δ_σ and Δ_π . The gap functions $\Delta_{\sigma,\pi}$ in MgB₂ in the Matsubara representation, suitable for the description of thermodynamic properties, were calculated in Ref. 10 from the solution of the Eliashberg equations using the theoretically calculated EPI spectral functions for the effective two-band model. Here we extend this approach to obtain the complex gap parameters $\Delta_{\sigma,\pi}(E)$ in MgB₂ as a functions of the real energy E . The results are shown in Fig. 1 and demonstrate the self-energy effects important for the description of the transport properties across MgB₂ point contacts. These effects reveal themselves via energy dependence of quasiparticle density of states and Andreev reflec-

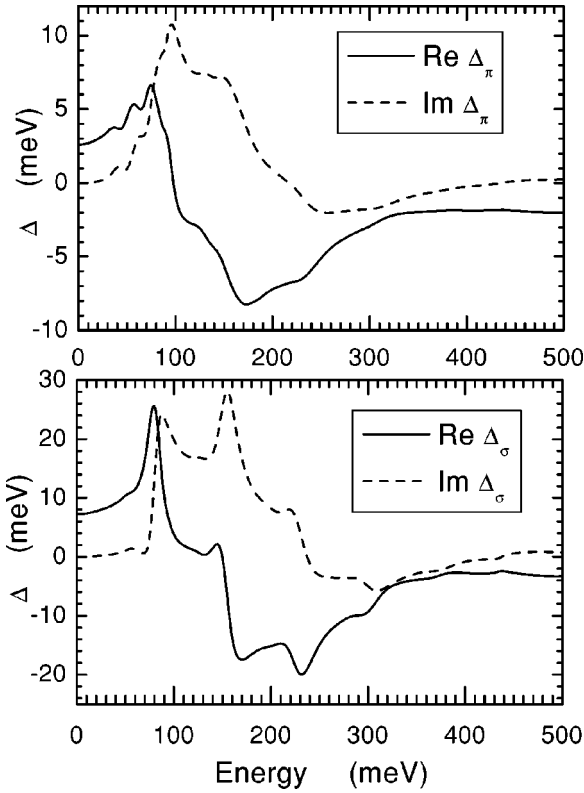


FIG. 1. The self-energy effects in the complex order parameter of superconducting MgB_2 . The upper and lower panels are for the π -band and the σ -band, respectively.

tion processes in point contacts with tunneling and direct conductivity current, correspondingly.

If the point contact is clean, then the electron mean free path l is greater than the size of the constriction d , and the current flows in the ballistic regime. The differential conductance of S - c - N contact at $T=0$ obeys the following expression:¹¹

$$\left(\frac{dI}{dV}\right)_{bal} = \frac{1}{R_N} \left(1 + \left| \frac{\Delta(\epsilon)}{\epsilon + \sqrt{\epsilon^2 - \Delta^2(\epsilon)}} \right|^2 \right) \epsilon = eV, \quad (1)$$

where R_N is the normal state resistance.

In the dirty contact ($l \ll d$), the regime of current flow is diffusive and the corresponding expression for the differential conductance follows from formula (21) from Ref. 12 for the current-voltage dependence:

$$I(V) = \frac{V}{R_N} + \frac{1}{eR_N} \int_0^{eV} d\epsilon \times \left[\text{Re} \frac{u}{\sqrt{u^2 - 1}} \left(\frac{\text{Re} \text{arcsinh} \left(\frac{1}{\sqrt{u^2 - 1}} \right)}{\text{Re} \left(\frac{1}{\sqrt{u^2 - 1}} \right)} \right) - 1 \right], \quad (2)$$

where $u = \epsilon/\Delta(\epsilon)$, $\epsilon = eV$, which yields

$$\left(\frac{dI}{dV}\right)_{dif} = \frac{1}{2R_N} \ln \left| \frac{\epsilon + \Delta(\epsilon)}{\epsilon - \Delta(\epsilon)} \right| \times \left[\text{Re} \frac{\epsilon}{\sqrt{\epsilon^2 - \Delta^2(\epsilon)}} / \text{Re} \frac{\Delta(\epsilon)}{\sqrt{\epsilon^2 - \Delta^2(\epsilon)}} \right], \quad \epsilon = eV. \quad (3)$$

It is well known that in the tunnel regime the differential conductance is proportional to the quasiparticle density of states:⁴

$$\left(\frac{dI}{dV}\right)_{tun} = \frac{1}{R_N} \text{Re} \frac{\epsilon}{\sqrt{\epsilon^2 - \Delta^2(\epsilon)}}, \quad \epsilon = eV. \quad (4)$$

We assume $T=0$ in these formulas, but they can be generalized to a finite temperature as well.

These formulas acquire a very simple form in the limit $eV \gg \Delta$. For tunnel, ballistic and diffuse point contacts they are as follows:

$$\left(\frac{dI}{dV}\right)_{tun} \approx \frac{1}{R_N} \left[1 + \frac{\text{Re}^2 \Delta(\epsilon)}{2\epsilon^2} - \frac{\text{Im}^2 \Delta(\epsilon)}{2\epsilon^2} \right], \quad (5)$$

$$\left(\frac{dI}{dV}\right)_{bal} \approx \frac{1}{R_N} \left[1 + \frac{\text{Re}^2 \Delta(\epsilon)}{4\epsilon^2} + \frac{\text{Im}^2 \Delta(\epsilon)}{4\epsilon^2} \right], \quad (6)$$

and

$$\left(\frac{dI}{dV}\right)_{dif} \approx \frac{1}{R_N} \left[1 + \frac{\text{Re}^2 \Delta(\epsilon)}{3\epsilon^2} \right], \quad (7)$$

where $\epsilon = eV$, respectively. Thus, the dI/dV characteristics of any point contact (tunnel, ballistic, diffusive) are roughly similar below 80 meV, where the contribution of $\text{Im}\Delta(\epsilon)$ is negligible.

In order to compare the theoretical predictions with the experimental spectra we express the calculated spectra as the second harmonic [i.e., rms voltage, $V_2(V)$] of the small first harmonic modulation voltage V_1 by expanding the $V(I)$ characteristic in the Taylor series. Namely, we express the V_2 signal as

$$V_2(V) \approx -\frac{V_1^2}{2\sqrt{2}} \frac{d}{dV} \left(R_N \frac{dI}{dV} \right), \quad (8)$$

assuming that changes in differential resistance is small and, correspondingly, the modulation voltage is fixed at V_1 . Any other spectra can be reduced to the particular value of V_1 using Eq. (8). In what follows we choose $V_1 = 3$ meV, which is close to the value used in the experiments.

In Figs. 2(a) and 2(b) the second harmonic voltages $V_2(V_1 = 3 \text{ meV})$ calculated by formulas (5)–(8) are shown for the π bands and σ bands of MgB_2 . These extreme regimes of current flow: tunnel, ballistic, and diffusive, are calculated using $\Delta(eV)$ functions from Fig. 1. One can see a small amplitude (of the order of 1 μV) of the phonon structure for the π -band, and a much stronger E_{2g} phonon mode singularity at about 80 meV for the σ -band. Up to $eV \approx 80$ meV the self-energy structure is determined by

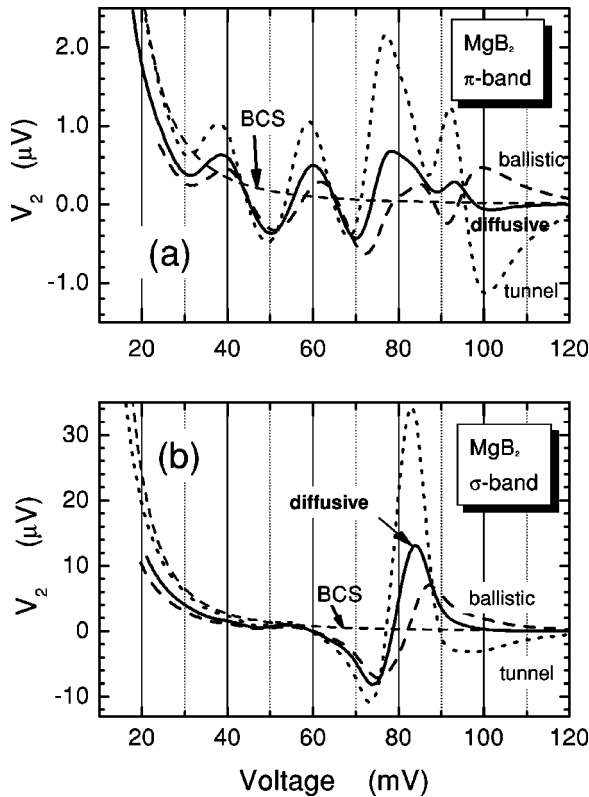


FIG. 2. The calculated second harmonic signal $V_2(V)$ proportional to the second derivative of the I - V -characteristic of the N - c - S point-contact with a ballistic or a diffusive regime of current flow (see text). For comparison, the corresponding curve for the tunnel junction N - I - S is shown together with the BCS tunneling density of states. Calibration of V_2 is reduced to modulation voltage $V_1 = 3$ mV.

$\text{Re}\Delta(\epsilon)$. The amplitude of phonon structure is different, reflecting the corresponding prefactors $1/2 \rightarrow 1/3 \rightarrow 1/4$ in the row of current flow regimes: tunnel \rightarrow diffusive \rightarrow ballistic. On the other hand, large differences in shape are observed in

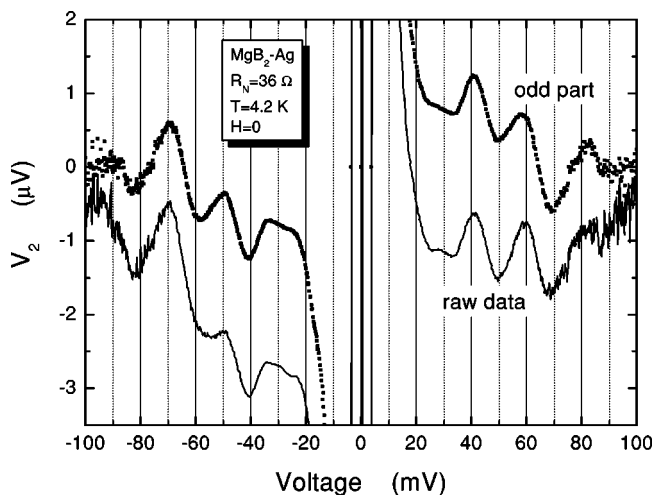


FIG. 3. The extraction of an odd part of the experimental point-contact spectra shown for the middle curve in Fig. 4(a). The thinner curve shows the raw data shifted vertically down for clarity.

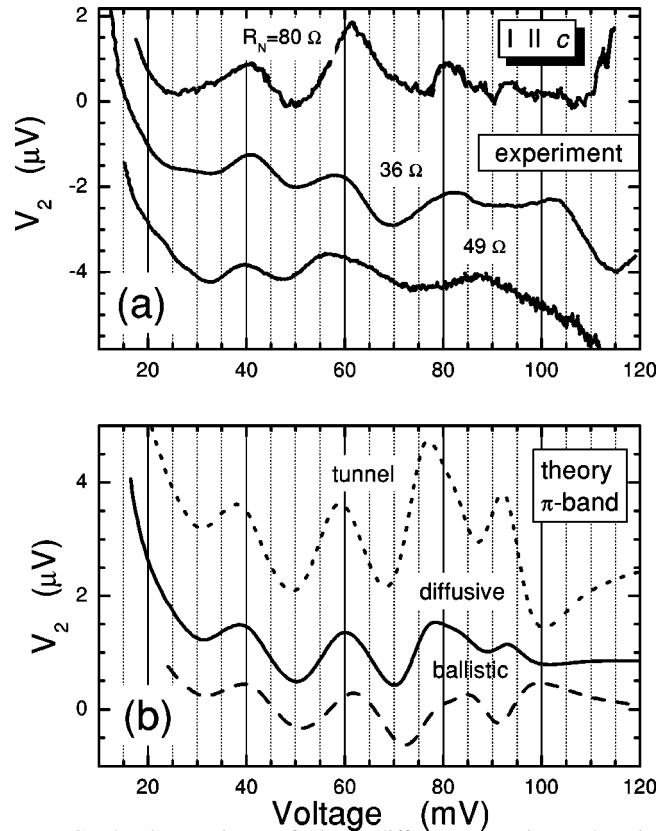


FIG. 4. Comparison of three different experimental point-contact spectra [panel (a)] in the c direction (Ref. 7) with the theoretical ones [panel (b)] calculated by asymptotic formulas (5)–(8) based on superconducting order parameter $\Delta(\epsilon)$ from Fig. 1. All the curves are displaced vertically for clarity and reduced to modulation voltage $V_1 = 3$ mV. In panel (a), the normal state resistances 49 and 36Ω correspond to zero-bias $R_0 = 45\Omega$ and 43Ω , respectively, being the same as in Fig. 2 (b) of Ref. 7. For $R_N = 80\Omega$ $R_0 = 150\Omega$. The experimental curves are smoothed by several mV not disturbing the phonon structure, $T = 4.2$ K, $H = 0$.

the energy range 80–120 meV, where $\text{Im}\Delta(\epsilon)$ becomes appreciable. We shall see below that just at the high-energy edge the experimental curves show some variation due to the uncontrollable changes of scattering in the contact region. We checked that for MgB_2 in c direction with the energy gap of about 2 meV the asymptotic formulas (5)–(7) almost completely coincide with the exact ones (1), (3), and (4) in the phonon energy range.

III. COMPARISON WITH EXPERIMENT

Since the theoretical spectra are odd with regard to the changes of the dc voltage sign, we extract the odd part of the raw data as shown in Fig. 3:

$$V_2^{\text{odd}} = \frac{1}{2}[V_2(eV) - V_2(-eV)]. \quad (9)$$

In Fig. 4 we compare three odd parts of the experimental spectra for different point contacts which are perpendicular to the surface of the c -oriented thin film.¹³ The superconducting energy gaps Δ_0 measured by the Andreev reflection spectroscopy from dV/dI characteristic lie in the range 2.1–2.6

meV. These dV/dI curves show almost no traces connected with the large gap at about 7 meV. Hence, for this orientation we probe only the π -band.⁸ We compare the experimental curves [Fig. 4(a)] with the π -band calculated spectra [Fig. 4(b)], since in the experiments the regime of current flow is among the extremes calculated by the theory. One can see that not only the shape of the experimental spectra corresponds well to the theoretical ones (with minor deviations), but also the amplitude of the structure has a proper order of magnitude ($\sim 0.1\%$ of R_N). From the $dV/dI(V)$ Andreev reflection spectra (see the caption in Fig. 4) one can suggest that our contacts are closer to the tunnel regime in the series of the experimental curves with resistances $49 \rightarrow 36 \rightarrow 80 \Omega$. To make the estimation more quantitative, one needs an interpolation formula similar to the finite barrier parameter Z in the Blonder-Tinkhan-Klapwijk theory.¹⁴

The question arises as to why we did not observe a much stronger self-energy S -type structure in Ref. 15, where the point-contact spectrum of MgB_2 single crystal was measured along ab plane? The answer is that in that case the nonequilibrium phonon generation is so strong that superconductivity in the contact region is destroyed, and correspondingly, the excess current dramatically decreases around the E_{2g} phonon mode energy. This leads to a large maximum in the $dV/dI(V)$ characteristic and the N-shape singularity in $V_2(V)$. The maximum can be easily seen in the $V_1(V)$ characteristic (note, for example, the inset in Fig. 1 of Ref. 15). Normally, this destruction of superconductivity masks the self-energy structure effectively. It can be identified by the strong dependence of energy position on external parameters: magnetic field and temperature.

IV. SUMMARY

In conclusion, we have derived the simple asymptotic formulas for the order parameter self-energy effects in the superconducting point contact. In MgB_2 with a short mean free path (diffusive point contact), the self-energy effects reveal themselves as the only peculiarities at phonon energies in the voltage dependence of the excess current, since the inelastic backscattering current, on which the traditional point-contact spectroscopy is based, is negligibly small. They can be used in standard programs^{16,17} to solve the Eliashberg equations⁴ for quantitative derivation of electron-phonon-interaction spectral function providing the structure of point-contact is established. In MgB_2 , we applied them in c direction for obtaining point-contact spectra in π band. The close similarity between the calculated and measured point-contact spectra in the c -direction manifests the validity of the calculated EPI spectral function in the π band in Ref. 10.

ACKNOWLEDGMENTS

The authors are grateful to N. L. Bobrov and V. V. Fisun for their collaboration in the MgB_2 investigation. O.V.D. and A.A.G. thank S. V. Shulga for the help in numerical calculations. S. I. Beloborod'ko is grateful to A. N. Omel'yanchuk for discussion. The work in Ukraine was carried out in part by the State Foundation of Fundamental Research under Grant No. $\Phi 7/528-2001$.

*Corresponding author. Email address: yanson@ilt.kharkov.ua

¹Jun Nagamatsu, Norimasa Nakagawa, Takahiro Muranaka, Yuji Zenitani, and Jun Akimitsu, *Nature (London)* **410**, 63 (2001).

²I.I. Mazin and V.P. Antropov, *Physica C* **385**, 49 (2003).

³H.J. Choi, M.L. Cohen, and S.G. Louie, *Physica C* **385**, 66 (2003).

⁴E.L. Wolf, *Principles of Electron Tunneling Spectroscopy* (Oxford University Press, London, 1985).

⁵O.V. Dolgov, R.S. Gonnelli, G.A. Ummarino, A.A. Golubov, S.V. Shulga, and J. Kortus, *Phys. Rev. B* **68**, 132503 (2003).

⁶A.I. D'yachenko, Y.Yu. Tarenkov, A.V. Abal'oshev, and S.J. Lewandowski, cond-mat/0201200 (unpublished).

⁷I.K. Yanson, V.V. Fisun, N.L. Bobrov, Yu.G. Naidyuk, W.N. Kang, Eun-Mi Choi, Hyun-Jung Kim, and Sung-Ik Lee, *Phys. Rev. B* **67**, 024517 (2003).

⁸A. Brinkman, A.A. Golubov, H. Rogalla, O.V. Dolgov, J. Kortus, Y. Kong, O. Jepsen, and O.K. Andersen, *Phys. Rev. B* **65**, 180517 (2002).

⁹I.I. Mazin, O.K. Andersen, O. Jepsen, A.A. Golubov, O.V. Dolgov, and J. Kortus, *Phys. Rev. B* **69**, 056501 (2004).

¹⁰A.A. Golubov, J. Kortus, O.V. Dolgov, O. Jepsen, Y. Kong, O.K.

Andersen, B. Gibson, K. Ahn, and R.K. Kremer, *J. Phys.: Condens. Matter* **14**, 1353 (2002).

¹¹A.N. Omelyanchuk, S.I. Beloborod'ko, and I.O. Kulik, *Fiz. Nizk. Temp.* **14**, 1142 (1988) [*Sov. J. Low Temp. Phys.* **14**, 630 (1988)].

¹²S.I. Beloborod'ko and A.N. Omelyanchuk, *Fiz. Nizk. Temp.* **17**, 994 (1991) [*Sov. J. Low Temp. Phys.* **17**, 518 (1991)].

¹³W.N. Kang, Hyeong-Jin Kim, Eun-Mi Choi, C.U. Jung, and Sung-Ik Lee, *Science* **292**, 1521 (2001). W.N. Kang, Eun-Mi Choi, Hyeong-Jin Kim, Hyun-Jung Kim, and Sung-Ik Lee, *Physica C* **385**, 24 (2003).

¹⁴G.E. Blonder, M. Tinkham, and T.M. Klapwijk, *Phys. Rev. B* **25**, 4515 (1982).

¹⁵Yu.G. Naidyuk, I.K. Yanson, O.E. Kvitnitskaya, S. Lee, and S. Tajima, *Phys. Rev. Lett.* **90**, 197001 (2003).

¹⁶W.L. McMillan and J.M. Rowell, *Phys. Rev. Lett.* **14**, 108 (1965).

¹⁷A.A. Galkin, A.I. D'yachenko, and V.M. Svistunov, *Zh. Eksp. Teor. Fiz.* **66**, 2262 (1974) [*Sov. Phys. JETP* **39**, 1115 (1974)]; V.M. Svistunov, A.I. D'yachenko, and M.A. Belogolovskii, *J. Low Temp. Phys.* **31**, 339 (1978).